JACS
JOURNAL OF THE AMERICAN CHEMICAL SOCIETY
Article
pubs.acs.org/JACS

Radical Cation and Neutral Radical of Aza-thia[7]helicene with SOMO−HOMO Energy Level Inversion

Ying Wang,[†,§] Hui Zhang,[†,§] Maren Pink,[‡] Arnon Olankitwanit,[†] Suchada Rajca,[†] and Andrzej Rajca*[,†]

[†]Department of Chemistry, University of Nebraska, Lincoln, Nebraska 68588-0304, United States
[‡]Department of Chemistry, Indiana University, Bloomington, Indiana 47405-7102, United States

Supporting Information

ABSTRACT: We report a relatively persistent, open-shell aza-thia[7]-helicene with cross-conjugated electron-rich π-system. The singly occupied molecular orbital (SOMO) energy levels of both radical cation and neutral radical of the [7]helicene are below the highest occupied molecular orbital (HOMO) energy levels, thereby violating the Aufbau principle. The aza-thia[7]helicene is prepared from β-hexathiophene by a three-step one-pot reaction, in which the pyrrole ring is constructed by two consecutive C−N bond formations. Chemical oxidation converts the helicene to its radical cation, while in the presence of base (Cs_2CO_3), the oxidation gives neutral aminyl radical, likely via proton dissociation from the aminium radical cation with a low pK_a. Reaction of the aza-thia[7]helicene with NaH provides the corresponding anion, which shows characteristic cyclic voltammetry wave at anodic peak potential $E_p^a \approx +0.2$ V. Chemical oxidation of the anion with ferrocenium hexafluorophosphate at room temperature gives persistent neutral aminyl radical. Structure of the aza-thia[7]helicene is supported by NMR, IR, X-ray crystallography, and cyclic voltammetry. The radical cation and neutral radical are characterized by EPR and UV−vis-NIR spectroscopies. DFT computations of the radical cation and neutral radical predict the SOMO−HOMO energy level inversion, which is supported experimentally by electrochemical data for the radical cation.

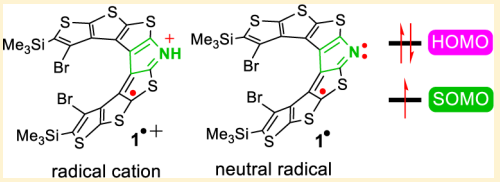

INTRODUCTION

Open-shell organic molecules with helical structure possess a combination of unique and intriguing characteristics that are not only of fundamental interest but also could have significant technological applications. Organic radicals have played an important role in chemistry, biochemistry, material sciences, and biomedicine, while aesthetically pleasing, helical structures are among the most fascinating chiral motifs.[1] There are only a few known open-shell helical molecules, with the majority of them being radical ions of relatively short helical structures,[1] except a helical diazaphenalenyl neutral radical (and a related [4]helicene neutral radical and [5]helicene singlet biradical) and a radical cation of thia[7]helicene, [7]Th$^{\bullet+}$ (Figure 1).[2−5] Difficulties in the synthesis and radical generation, as well as in handling reactive radical species, are among the factors deterring widespread attention to this fascinating class of organic molecules.

Recent resurgence of interest in [*n*]helicenes, *ortho*-annelated polycyclic aromatic molecules with nonplanar helical conjugation of the π-electron system, has revitalized the efforts to develop more efficient synthetic methods and expansive applications.[1] [*n*]Helicenes have become more accessible and modern synthetic methodologies have provided a variety of new [*n*]heterohelicenes, in which the embedded heteroatom(s) could provide additional functionalities.[1,6−12] While these developments greatly facilitate the design and synthesis of open-shell [*n*]helicene molecules, the detrimental reactivity of open-shell species remains the biggest impediment. The common, effective strategy for stabilizing open-shell species is to shield the radical site using bulky substituents, but it may be difficult to implement, as well as unappealing, in the design and synthesis of [*n*]helicenes. An alternative strategy, which relies on decreasing spin density at the radical site by resonance delocalization, would be more amiable to open-shell [*n*]-heterohelicenes.

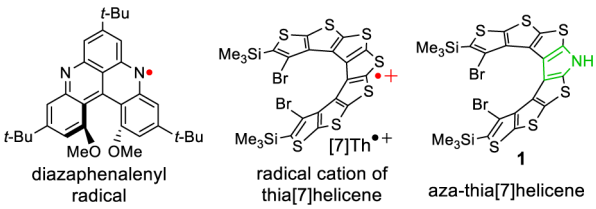

Figure 1.

With our recent preparation of thia[7]helicene radical cation as beneficial groundwork,[2] we explore the design and synthesis of new stable open-shell [*n*]heterohelicenes. We draw upon the aza-thia[7]helicene **1** (Figure 1), an analogue of thia[7]-helicene, in which the center thiophene ring is replaced with the pyrrole, as the precursor for the generation of nitrogen-centered radical (aminyl) and radical cation. Presumably, the stability of the open-shell aza-thia[7]helicene would be enhanced by the sulfur heteroatoms in close proximity. Both experimental and computational studies provide valuable

Received: February 9, 2016
Published: May 24, 2016

DOI: 10.1021/jacs.6b01498
J. Am. Chem. Soc. 2016, 138, 7298−7304

insight into electronic properties of these open-shell [7]-helicenes.

Here we disclose the distonic radical cation[13] of aza-thia[7]helicene, as well as the neutral radical. In both molecules, electronic configurations violate the Aufbau principle. For an open-shell molecule, the Aufbau principle dictates that the singly occupied molecular orbital (SOMO) is above the doubly occupied highest-energy occupied molecular orbital (HOMO). Formal violation of this principle, such as the SOMO−HOMO energy-level inversion phenomenon, is of fundamental interest.[14−18]

RESULTS AND DISCUSSION

Aza-thia[7]helicene **1** is prepared from β-hexathiophene **2** by a three-step one-pot reaction, in which the pyrrole ring is constructed by two consecutive C−N bond formations (Scheme 1).

Scheme 1

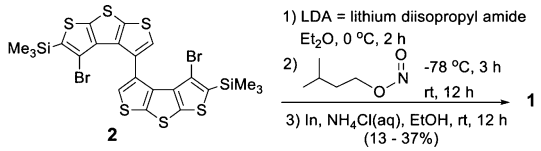

In the first step, **2** is dilithiated with LDA at the two α-positions of thiophene,[19,20] and then the resultant dilithio compound is reacted with isopentyl nitrite to provide intermediate hydroxylamine. In the third step, the hydroxylamine is reduced to secondary amine using indium metal[21] to provide [7]helicene **1**. The ^{1}H and ^{13}C NMR spectra provide evidence for 2-fold symmetric structure of **1**, while ^{1}H−^{15}N HSQC and IR spectra ($\nu \approx 3370$ cm^{-1}) confirm the presence of the N−H moiety. In particular, ^{15}N chemical shift $\delta = -266$ ppm is in agreement with the DFT-computed $\delta = -261$ ppm for **1** (ref 0 ppm for CH_3NO_2).[22,23] The [7]helicene structure of **1** was confirmed by single-crystal X-ray analysis (Figure 2).

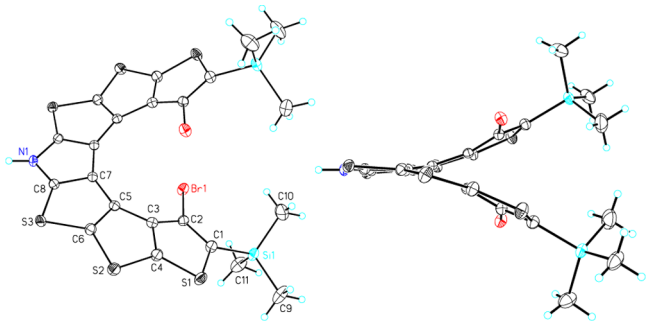

Figure 2. Molecular structure and conformation for aza-thia[7]-helicene **1**. Carbon, nitrogen, sulfur, bromine, and silicon atoms are depicted with thermal ellipsoids set at the 50% probability level. Further details are reported in Tables S1 and S2 and Figure S1, SI.

Cyclic voltammetry of **1** in 0.1 M tetrabutylammonium hexafluorophosphate ($[n\text{-Bu}_4\text{N}]^+[\text{PF}_6]^-$) in dichloromethane (DCM) shows a reversible wave at $E_1^\circ = +0.884 \pm 0.010$ V (mean ±1 std dev), which is followed by the second, not fully reversible, wave at $E_2^\circ = +1.086 \pm 0.005$ V (Figure 3). Both waves appear significantly below $E_1^\circ = +1.34$ V and $E_2^\circ = +1.82$ V for thia[7]helicene, [7]Th.[19] The first, reversible, wave and

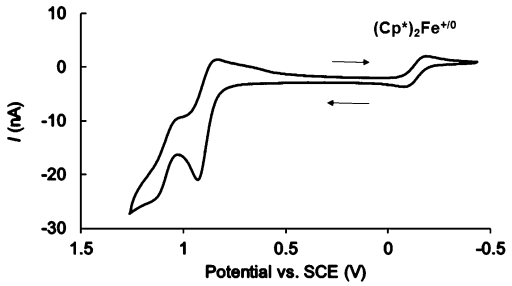

Figure 3. Cyclic voltammogram at 100 mV s^{-1} for aza-thia[7]helicene **1** in 0.1 M $[n\text{-Bu}_4\text{N}]^+[\text{PF}_6]^-$ in DCM and internally referenced to $\text{Cp}^*_2\text{Fe}^{+/0}$ in DCM (−0.130 V vs SCE). Further details are reported in Table S3 and Figures S2 and S3, SI.

the second wave most likely correspond to a one-electron oxidation of **1** to its radical cation ($\mathbf{1}^{\bullet+}$) and to a two-electron oxidation to its diradical dication ($\mathbf{1}^{2\bullet 2+}$), respectively.[24] Therefore, nitrosonium hexafluorophosphate $[\text{NO}]^+[\text{PF}_6]^-$ in DCM ($E^\circ = +1.40$ V in DCM)[25] should be an effective oxidant for the oxidation of **1** to its radical cation ($E_1^\circ \approx +0.9$ V).

We explored chemical oxidation of **1** in which all experiments are carried out in a custom-made Schlenk vessel designed for in situ EPR or EPR and UV−vis−NIR spectroscopic measurements to monitor the oxidation process (Scheme 2).[2]

Scheme 2. Generation of Radicals $\mathbf{1}^{\bullet+}\text{PF}_6^-$ and $\mathbf{1}^{\bullet}$

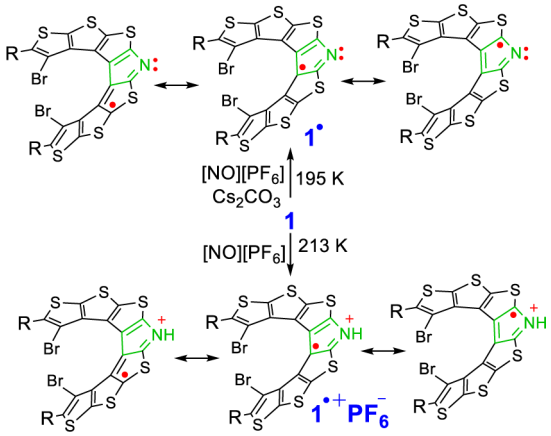

A brief exposure of **1** in DCM to solid $[\text{NO}]^+[\text{PF}_6]^-$ at low temperature (213 K) provided a green-yellow colored reaction mixture, which was immediately decanted into the cell compartment for EPR measurement at 233 K. The EPR spectrum showed a broad $I = 1$ triplet with ^{14}N-hyperfine splitting, $a_N = 0.23$ mT, and isotropic g-value, $g = 2.005$, that was assigned to radical cation $\mathbf{1}^{\bullet+}\text{PF}_6^-$ (Figure 4).

This finding is in agreement with the DFT-computed spectrum of C_2-symmetric $\mathbf{1}^{\bullet+}$, using the UB3LYP/6-31G(d,p) method and IEF-PCM-UFF solvent model for dichloromethane.[23] In particular, $a_N = 0.168$ and $a_H = 0.053$ mT were computed, thus suggesting that ^{1}H hyperfine splittings are unresolved in the experimental spectrum (line-width ≈ 0.16 mT). The calculated C_2-symmetric structure of $\mathbf{1}^{\bullet+}$ has a significant fraction of spin density, ~0.33 unpaired electrons, at heavy atoms, such as sulfur atoms, similar to that observed for sulfur-rich radical cations, including $[7]\text{Th}^{\bullet+}$ (Table S9, SI).[2,26] Thus, the g-value for $\mathbf{1}^{\bullet+}$ is expected to be similar to that for $[7]\text{Th}^{\bullet+}$ ($g = 2.006$),[2] which is significantly greater than those

DOI: 10.1021/jacs.6b01498
J. Am. Chem. Soc. 2016, 138, 7298−7304

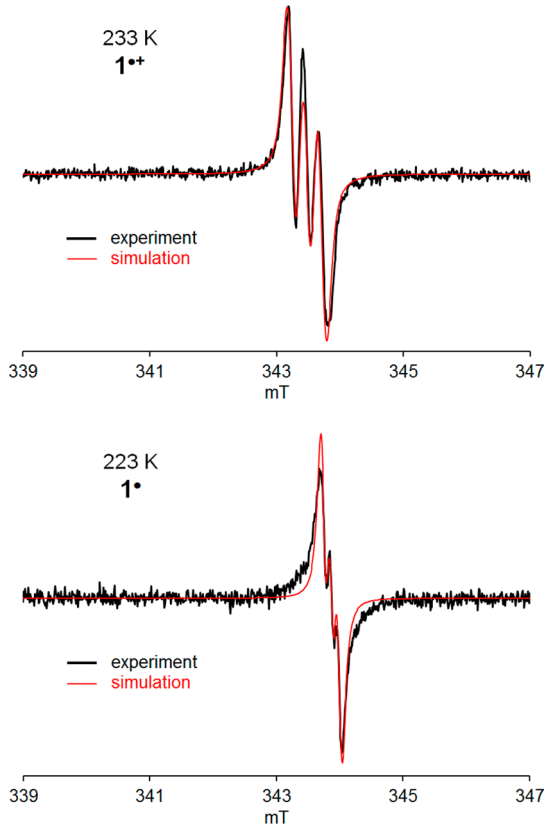

Figure 4. EPR spectra obtained during oxidation of **1** with $[NO]^+[PF_6]^-$ showing radical cation $\mathbf{1}^{\bullet+}PF_6^-$ (ν = 9.6397 GHz) and during the oxidation in the presence of base (Cs_2CO_3) showing aminyl radical $\mathbf{1}^{\bullet}$ (ν = 9.6568 GHz). Spectral simulations correspond to the following parameters: $\mathbf{1}^{\bullet+}PF_6^-$, a_N = 0.23 mT, g = 2.0050, line-width = 0.16 mT; $\mathbf{1}^{\bullet}$, a_N = 0.12 mT, g = 2.0040, line-width = 0.085 mT.

for the radical cation of alkyl-substituted α-sexithiophene (g = 2.0023) and typical N-centered (aminium) radical cations (g = 2.003).[26,27] Furthermore, EPR spectra of $\mathbf{1}^{\bullet+}PF_6^-$ remain intense at low temperatures for at least 1 h, providing evidence for its persistence.

The helical shape and large terminal substitution are likely the determinant of the low propensity for formation of diamagnetic π-dimers of $\mathbf{1}^{\bullet+}PF_6^-$ and $[7]Th^{\bullet+}PF_6^-$.[2] This is in contrast to the radical cations of α-oligothiophenes, in which their EPR signal mostly disappears at low temperature, due to formation of diamagnetic π-dimers.[28]

We explored the possibility of generating neutral aminyl radical $\mathbf{1}^{\bullet}$ via in situ formation of $\mathbf{1}^{\bullet+}$ followed by a proton transfer from the NH group of $\mathbf{1}^{\bullet+}$ to a weak base such as Cs_2CO_3 (Scheme 2). This transfer should be facilitated by the acidity of $\mathbf{1}^{\bullet+}$; for example, the carbazole radical cation was reported to possess pK_a of 1.5.[29] Because the neutral radical $\mathbf{1}^{\bullet}$ is expected to be less stable than $\mathbf{1}^{\bullet+}$, the generation of $\mathbf{1}^{\bullet}$ should occur at lower temperature.

When the oxidation of **1** is carried out in the presence of a large excess (6+ equiv) of cesium carbonate, Cs_2CO_3, at low temperature (195 K), the observed EPR spectrum at 223 K is much narrower and upfield shifted, with $a_N \approx 0.1$ mT and g = 2.004, compared with that of the radical cation. With the aid of computation, we assign this EPR spectrum to a neutral aminyl radical $\mathbf{1}^{\bullet}$ (Figure 3). The UB3LYP/6-31G(d,p)-IEF-PCM-UFF+ZPVE computations[23] for C_2-symmetric $\mathbf{1}^{\bullet}$ indicate smaller hyperfine splittings, a_N = 0.106 mT, and a smaller fraction of spin density located on sulfur atoms (~0.17 unpaired electrons), thus supporting the assignment to $\mathbf{1}^{\bullet}$, and, in particular, the decreased g-value vs that of radical cation.[26] These results are consistent with significant delocalization of spin density onto carbons of the fused ring [7]helicene moiety.

We also explored the generation of $\mathbf{1}^{\bullet}$ from the corresponding anion. The anion of **1** ($\mathbf{1}^-$) is generated by the treatment of aza-thia[7]helicene **1** with NaH in DCM/acetonitrile (DCM/MeCN) at room temperature. The electrochemical study of $\mathbf{1}^-$ at room temperature shows a characteristic cyclic voltammetry wave at an anodic peak potential of $E_p^a \approx +0.2$ V with a large peak-to-peak potential difference $E_p^a - E_p^c = 0.66 \pm 0.01$ V (mean ± SE) at scan rate of 0.2 V s^{-1}.[30] This implies a slow electron transfer process, which appears electrochemically irreversible. However, the observed return (cathodic) wave suggests that the process should be chemically reversible (Figure 5). Using the method of Kochi for such a case,[30] we estimated standard rate constant for the electron transfer, $k_s \approx 7 \times 10^{-7}$ cm s^{-1} (Table S4 and Figure S5, SI).[31] In THF at 294 K, the peak potential E_p^a for $\mathbf{1}^-$ overlaps that of decamethylferrocene (Cp^*_2Fe, $E_1^\circ \approx -0.13$ V, $E_p^a \approx -0.07$ V), while at low temperatures, such as 213 K, E_p^a for $\mathbf{1}^-$ shifts to

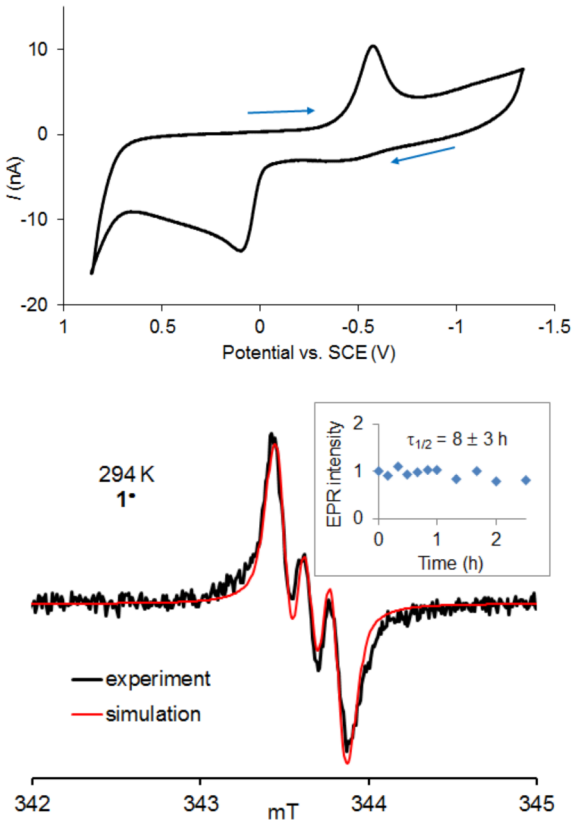

Figure 5. Study of anion of aza-thia[7]helicene **1**, obtained in a reaction of **1** with NaH at room temperature in DCM/MeCN. (top) Cyclic voltammogram at 200 mV s^{-1} for 0.3 mM anion of **1** in 0.08 M $[n\text{-}Bu_4N]^+[PF_6]^-$ in DCM/MeCN (1:3.5). (bottom and inset) EPR spectrum for $\mathbf{1}^{\bullet}$, obtained during oxidation of 0.4 mM anion of **1** with $[Cp_2Fe]^+[PF_6]^-$ in DCM/MeCN (20:1) at room temperature and EPR signal intensity vs time. Spectral simulation: a_N = 0.15 mT, g = 2.0032, line-width = 0.13 mT. Further details are reported in Table S4 and Figures S5, S6, and S9, SI.

DOI: 10.1021/jacs.6b01498
J. Am. Chem. Soc. 2016, 138, 7298−7304

higher potentials (+0.2 V), as expected for the slower electron transfer at low temperature. Interestingly, no return wave is found, up to a cathodic potential of about −1 V, when the experiment is carried out in THF at 213 K (Figure S6, SI).

The relatively low E_p^a and chemical reversibility in DCM/MeCN indicate that oxidation of the anion is feasible in this solvent mixture at room temperature. Indeed, the treatment of the anion of **1** (generated with NaH) with ferrocenium hexafluorophosphate at room temperature ($[Cp_2Fe]^+[PF_6]^-$, $E_1^\circ \approx +0.45$ V), a reliable, "innocent" one-electron oxidant,[25] provides the product corresponding to neutral aminyl radical **1**$^\bullet$, as indicated by EPR spectroscopy (Figure 5). Notably, the double-integrated EPR spectral intensity for **1**$^\bullet$ remained almost unchanged over the course of 2 h at room temperature; a numerical fit to the first order rate equation for the decay of the EPR signal gave a half-life, $\tau_{1/2} = 8 \pm 3$ h (mean ± SE) (Figure S9, SI).

We also treated aza-thia[7]helicene **1** with LDA to provide the anion **1**$^-$, which is then oxidized with $[Cp_2Fe]^+[PF_6]^-$. The EPR spectrum at 223 K with $g \approx 2.003$ of the product is similar to that for **1**$^\bullet$ in Figures 4 and 5 (Figure S10, SI).

We carried out the UV−vis-NIR measurements according to the previously reported procedure for thia[7]helicene.[2] Aza-thia[7]helicene **1** in DCM is briefly stirred with solid $[NO]^+[PF_6]^-$, and the reaction mixture is immediately decanted into the corresponding cell compartments for consecutive UV−vis-NIR and EPR measurements. The UV−vis−NIR spectrum shows an intense band at $\lambda_{max} = 370$ nm, a much weaker shoulder at 600 nm, and a broad weak band at 850−900 nm. The spectrum becomes more intense after additional exposure to $[NO]^+[PF_6]^-$. The solution shows an EPR spectrum at 295 K with $g \approx 2.003$ (Figure S8, SI), similar to that of **1**$^\bullet$ recorded earlier at 223−295 K.

Electronic UV−vis-NIR absorption spectra of the radical cation **1**$^{\bullet+}$ and the aminyl radical **1**$^\bullet$ are computed using the TD-UB3LYP/6-31G(d,p) method and IEF-PCM-UFF solvent model for DCM.[23] The calculated spectra for the C_2-symmetric structure of **1**$^\bullet$ qualitatively reproduce the band position at $\lambda_{max} = 370$ nm in the experimental spectra (Figure S8, SI). The exception is the mismatch of the broad NIR band at 850−900 nm, which may reflect the well-known deficiency of the TD-B3LYP method in the calculations of absorption bands with a large degree of charge transfer.[32]

The structures of **1**, **1**$^{\bullet+}$, and **1**$^\bullet$ with 2-fold symmetry (C_2) are computed at the B3LYP/6-31G(d,p)-IEF-PCM-UFF +ZPVE level of theory, employing both gas phase and IEF-PCM-UFF solvent models (cyclohexane for **1** and DCM for **1**$^{\bullet+}$ and **1**$^\bullet$). For **1**, a C_2-symmetric structure is found to be a minimum on the potential energy surface (PES); however, for **1**$^{\bullet+}$ and **1**$^\bullet$, C_2-symmetric geometries are unexpectedly found to be transition state (TS) structures (one imaginary frequency with $\bar{\nu} = i200-i300$ cm^{-1}). Following an intrinsic reaction coordinate (IRC) computation, it is found that these TS structures are intermediates between the two C_1-symmetric structures, which are a fraction of kcal mol^{-1} below the intermediates. When a zero-point vibrational energy (ZPVE) correction is included, the TS structures are lower in energy, thus suggesting that the overall structures for **1**$^{\bullet+}$ and **1**$^\bullet$ are fluxional and C_2-symmetric, in particular on a relatively slow time scale of the EPR spectroscopy. Upon distortion from C_2- to C_1-symmetric structures, representative spin density maps for C_2- and C_1-symmetric structures of **1**$^{\bullet+}$ and **1**$^\bullet$ show a significant redistribution of spin densities (Figure 6).

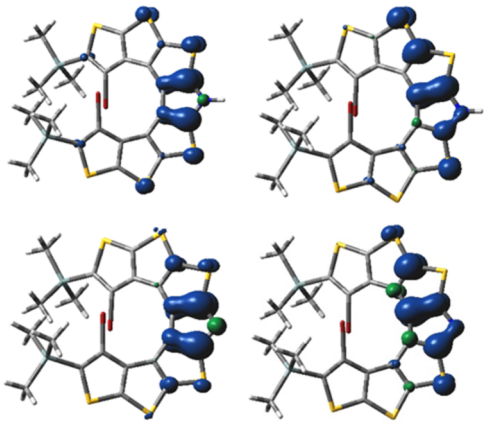

Figure 6. Spin density maps for **1**$^{\bullet+}$ (top) and **1**$^\bullet$ (bottom) for C_2- and C_1-symmetric structures at the UB3LYP/6-31G(d,p)-IEF-PCM-UFF +ZPVE level of theory (DCM). Positive (blue) and negative (green) spin densities are shown at the isodensity level of 0.004 electron/bohr.

Both C_2- and C_1-symmetric structures for **1**$^{\bullet+}$ have positive charge localized at the nitrogens, and the spin density is primarily localized at carbons, resembling distonic radical cations.[13] This finding is in contrast to thia[7]helicene radical cation [7]Th$^{\bullet+}$ and its analogous oxa-thia[7]helicene radical cation, for which, C_2-symmetric structures are minima on the PES.[2]

Most notably, the SOMO energy levels of the distonic-like radical cation **1**$^{\bullet+}$ and neutral radical **1**$^\bullet$ are below the doubly occupied HOMO energy levels, which violate the Aufbau principle (Figure 7).

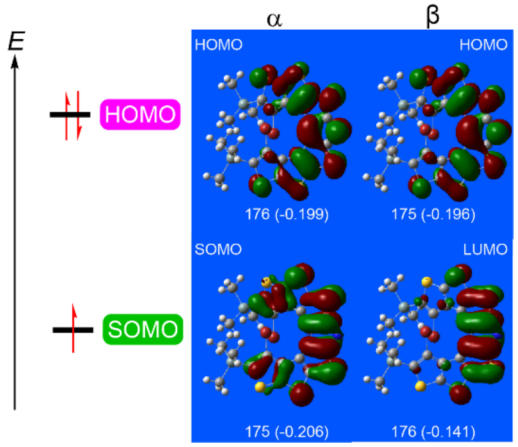

Figure 7. Orbital maps for the C_2-symmetric structure of **1**$^\bullet$ at the UB3LYP/6-31G(d,p)-IEF-PCM-UFF+ZPVE level of theory (DCM). Positive (red) and negative (green) contributions are shown at the isodensity level of 0.02 electron/bohr. The singly occupied α orbital is matched in a nodal pattern to the lowest unoccupied β orbital to provide the SOMO energy level; doubly occupied molecular orbitals, including the HOMO, are identified by matching nodal patterns and energies (in hartrees) of the α and β occupied orbitals.

These orbital configurations are even maintained in polar solvents such as dimethyl sulfoxide (DMSO) and water, as well as when employing dispersion corrected DFT (Tables S12A−C, SI).[33−36] In addition, we found that the N−H bond dissociation energy in **1** is increased by only ~0.5 kcal mol^{-1} in water, compared with that in DCM at the UM06-2X/6-31G(d,p)-IEF-PCM-UFF+ZPVE level of theory (Table

DOI: 10.1021/jacs.6b01498
J. Am. Chem. Soc. 2016, 138, 7298−7304

6B,SI).[16,35] This is in contrast to the recently investigated radical anions, with an inversion of the SOMO and HOMO energy levels, in which the stabilizing effect of the anion on the radical was significantly diminished in polar solvents.[16,17]

The computed inversion of the SOMO and HOMO energy levels in radical cation $\mathbf{1}^{\bullet+}$ correlate well with the voltammetry of **1** with the relatively small difference between E_2° and E_1° of ca. 0.2 V (Figure 3, and the SI: Table S3 and Figures S2 and S3).[24] Note that the difference between E_2° and E_1° for thia[7]helicene, [7]Th, is about 0.5 V and the computed orbital configurations for [7]Th$^{\bullet+}$, as well as the analogous radical cation of oxa-thia[7]helicene, obey the Aufbau principle (Tables S7 and S14, SI).

For comparison, we investigated "[3]helicene" homologues of $\mathbf{1}^{\bullet+}$ and $\mathbf{1}^{\bullet}$ (Chart 1) and find that their SOMO−HOMO energy levels follow the Aufbau principle, even though these lower homologues also display analogous PES, with C_{2v} TS structures and C_s minima (Tables S8 and S13, SI).

Chart 1. "[3]Helicene" Homologues of $\mathbf{1}^{\bullet+}$ and $\mathbf{1}^{\bullet}$

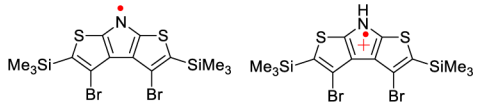

We rationalize that these observations may be associated with structures of the aza-thia[7]helicenes $\mathbf{1}^{\bullet+}$ and $\mathbf{1}^{\bullet}$. The electron-deficient pyrrole moiety imbedded in an extended, cross-conjugated [7]helicene π-system of relatively electron-rich thiophene rings provides a structure that may be viewed as approximately isoelectronic with distonic radical anion.[14−16]

We consider that the observed SOMO−HOMO energy level inversion in $\mathbf{1}^{\bullet+}$ and $\mathbf{1}^{\bullet}$ coupled with the cross-conjugated [7]helicene structure may provide a novel avenue to high-spin ground states for the corresponding $\mathbf{1}^{2\bullet2+}$ and $\mathbf{1}^{2\bullet+}$ (Figure 8).[14]

Our DFT computations indicate that both $\mathbf{1}^{2\bullet2+}$ and $\mathbf{1}^{2\bullet+}$ in DCM possess nearly degenerate nondisjoint SOMOs[37] (energies within 0.005 au) and triplet ground states with singlet triplet energy gaps (ΔE_{ST}) of about 2 kcal mol^{-1}.[38]

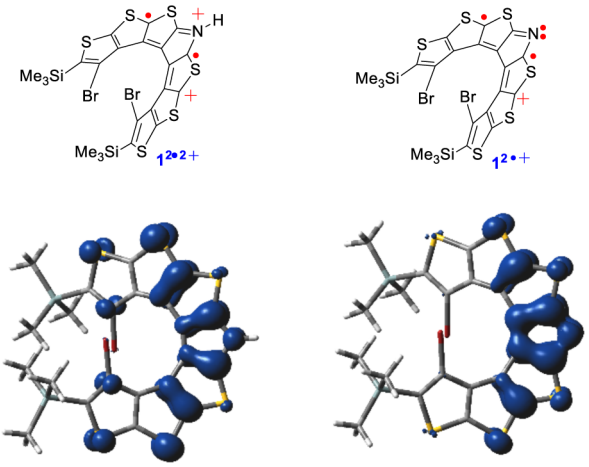

Figure 8. Structure drawings and spin density maps for the C_2-symmetric ground state triplet diradicals: $\mathbf{1}^{2\bullet2+}$ (left) and $\mathbf{1}^{2\bullet+}$ (right). Positive (blue) and negative (green) spin densities are depicted at the isodensity level of 0.004 electron/bohr and were obtained at the UB3LYP/6-31G(d,p)-IEF-PCM-UFF+ZPVE level of theory (DCM). Further details are reported in Tables S9 and S15, SI.

Notably, ΔE_{ST} is about the same (or slightly higher) for $\mathbf{1}^{2\bullet+}$ in water compared with that in DCM, which is consistent with the absence of solvent effects on the SOMO−HOMO energy level inversion in neutral radical $\mathbf{1}^{\bullet}$. However, our experimental attempts to generate $\mathbf{1}^{2\bullet+}$ using both $[NO]^+[PF_6]^-/Cs_2CO_3$ and the stronger oxidant WCl_6 ($E^\circ \approx +1.6$ V in DCM)[24] so far have not been successful.[24,39]

The triplet ground state of [7]helicene $\mathbf{1}^{2\bullet+}$ is particularly fascinating because of the predicted ΔE_{ST} of 2 kcal mol^{-1} and the fact that its structure formally corresponds to a nitrenium ion.[40] Except for the simple structure of NH_2^+,[41] all other experimentally known nitrenium ions exist in the singlet ground state, especially those aryl-substituted structures with bent CNC moieties similar to that of $\mathbf{1}^{2\bullet+}$.[40,42] Notably, the computed spin density for [7]helicene $\mathbf{1}^{2\bullet+}$ shows a localization on carbon atoms of the cross-conjugated π-system (Figure 8). Thus, $\mathbf{1}^{2\bullet+}$ is predicted to possess an exceptional triplet ground state.

According to DFT computations, the **1**-C_s, $\mathbf{1}^{\bullet+}$-C_s, $\mathbf{1}^{\bullet}$-C_1, and $\mathbf{1}^{2\bullet+}$-C_s TS structures for racemization[43] are 38.2, 37.4, 36.6, and 36.4 kcal mol^{-1} above their corresponding C_2-symmetric structures, and therefore [7]helicenes **1**, $\mathbf{1}^{\bullet+}$, $\mathbf{1}^{\bullet}$, and $\mathbf{1}^{2\bullet+}$ (triplet) are expected to be configurationally stable at room temperature. For comparison, we computed the [7]Th-C_s and [7]Th$^{\bullet+}$-C_s TS structures for racemization of thia[7]helicenes [7]Th and [7]Th$^{\bullet+}$, which are found to be 45.4 and 42.8 kcal mol^{-1} above their corresponding C_2-symmetric structures that are minima on the PES. This result is in qualitative agreement with an experimental barrier of $\Delta G^{\ddagger}$ = 39 kcal mol^{-1} for racemization of [7]Th in the solid state and with an experimentally determined configurational stability of [7]-Th$^{\bullet+}PF_6^-$ in DCM at room temperature.[2,19] The barriers for racemization of about 35 kcal mol^{-1} for [7]helicenes **1**, $\mathbf{1}^{\bullet+}$, $\mathbf{1}^{\bullet}$, and $\mathbf{1}^{2\bullet+}$ are within the lower limit for the free energy barrier for racemization in optoelectronic applications.[44,45] The combination of paramagnetism and configurationally stable helical π-system make the studied molecules promising prototypes for future studies of novel approaches to spintronics.[46,47]

EXPERIMENTAL SECTION

X-ray Crystallography. Crystal of **1** for X-ray studies was prepared by slow evaporation from solution in DCM at 4 °C. Data collection was performed at Indiana University using Mo Kα radiation (graphite monochromator). Final cell constants were calculated from the *xyz* centroids of 7124 strong reflections from the actual data collection after integration (SAINT).[48] The intensity data were corrected for absorption (SADABS).[49] The space group $C2/c$ was determined based on intensity statistics and systematic absences. The structure was solved using SIR-2004[50] and refined with SHELXL-97.[51] All non-hydrogen atoms were refined with anisotropic displacement parameters. The hydrogen atoms were placed in ideal positions and refined as riding atoms with relative isotropic displacement parameters. Crystal and structure refinement data for **1** are in the Supporting Information and the accompanying file in CIF format.

Synthesis of 1. Standard techniques for synthesis under inert atmosphere (argon or nitrogen), using custom-made Schlenk glassware, custom-made double manifold high vacuum lines, argon-filled Vacuum Atmospheres gloveboxes, and nitrogen-filled glovebags were followed. Chromatographic separations were carried out using normal phase silica gel, deactivated using 3% Et_3N in pentane.[52,53]

n-BuLi (1.625 M in hexane, 1.40 mL, 2.27 mmol) was added dropwise to a solution of diisopropylamine (0.35 mL, 2.48 mmol) in freshly distilled ether (6.4 mL) at 0 °C. After the reaction mixture had been stirred at 0 °C for 1 h, the resultant LDA solution (0.69 mL,

DOI: 10.1021/jacs.6b01498
J. Am. Chem. Soc. 2016, 138, 7298−7304

0.167 mmol, 2.3 equiv) was added to the starting material, bis(4,4′-dibromo-5,5′-di(trimethylsilyl)-dithieno[2,3-*b*:3′,2′-*d*]thiophene), that is, β-hexathiophene, **2** (50.2 mg, 72.9 μmol, 1.0 equiv), in dry ether (12 mL) under argon atmosphere at 0 °C.[19,20] After stirring at 0 °C for 2 h, the reaction mixture was placed in a −78 °C acetone−dry ice bath. Then freshly distilled isopentyl nitrite in ether (0.745 M, 120 μL, 89.4 μmol, 1.2 equiv) was added. The reaction mixture was kept at −78 °C for 3 h and then allowed to warm to ambient temperature and stirred overnight. The reaction mixture was transferred from the Schlenk vessel to a flask and concentrated under nitrogen gas flow. Then, to the flask the following reagents and solvents were added under the flow of nitrogen gas: degassed EtOH (3 mL), degassed saturated aqueous NH_4Cl (1.5 mL), and indium metal (10.6 mg, 92.3 μmol, 1.3 equiv).[21] The reaction mixture was stirred at ambient temperature overnight and then worked up with brine/ether, dried over sodium sulfate, and concentrated in vacuum. The residue was purified on silica gel flash column chromatography with 3% deactivated silica gel (ethyl acetate/pentane, 20:80) to give the product as a yellow powder (19.23 mg, 37%).

The product can further be purified by recrystallization from ether/pentane or DCM. For example, from four reactions on the 0.05 and 0.09 g scales, 51.9 mg (21%) of product was obtained from 243.8 mg of starting material after column. After additional recrystallization with ether/pentane, pure pale yellow crystals were collected (32.8 mg, overall yield 13%). Mp 272−274 °C (carbonized, under N_2). R_f = 0.46 (ethyl acetate/hexanes, 50:50, 4% deactivated TLC). ^{1}H NMR ($CDCl_3$, 700 MHz, ref 7.26 ppm for $CDCl_3$), δ = 8.64 (s, 1H), 0.41 (s, 18H). ^{1}H−^{15}N HSQC experiment (chloroform-*d*): crosspeak, ^{1}H δ = 8.640 ppm, ^{15}N δ = −265.79 ppm (ref 0 ppm for CH_3NO_2). ^{1}H NMR (acetone-d_6, 500 MHz), δ = 11.37 (s, 1H), 0.44 (s, 18H). ^{13}C NMR (acetone-d_6, 125 MHz), δ = 143.9, 141.9, 138.8, 136.1, 134.0, 129.5, 116.0, 114.0, −0.4. IR (ZnSe, cm^{-1}): 2953, 1465, 1406, 1395, 1248, 1049, 980, 956, 841, 758. MALDI-TOF-MS: (matrix 2,5-dihydroxybenzoic acid) found 704.8403. TOF-HRMS-EI (ion type, % RA for *m*/*z*): calcd for $C_{22}H_{19}Br_2NS_6Si_2$ at 704.7727 ($[M + 2]^+$, 100.0%), 702.7747 ($[M]^+$, 51.4%), 706.7706 ($[M + 4]^+$, 48.6%); found 704.7706 (100%, −3.0 ppm), 702.7735 (21%, −1.7 ppm), 706.7687 (51%, −0.3 ppm), respectively. UV/vis (cyclohexane): λ_{max}/nm (ε_{max}/L mol^{-1} cm^{-1}) = 242 (3.99×10^4), 333 (sh, $\sim 8 \times 10^3$), 409 ($\sim 4 \times 10^3$), 439 (sh, $\sim 3 \times 10^3$).

General Procedures for Electrochemical Studies. Electrochemical data for aza-thia[7]helicene **1** and its anion $\mathbf{1}^-$ in DCM or DCM/MeCN were obtained in a glovebag under argon gas atmosphere. Data for the anion in THF at 294 and 213 K were acquired in an argon-filled glovebox, equipped with a custom-made cold well for low temperature electrochemistry as described before.[54,55] The custom-made electrochemical cell with three electrodes was used (Ag-wire as quasi-reference, Pt-foil as counter, and a commercial 100-μm Pt-disk as working electrode). The cell was also equipped with a thin-wall glass capillary well for thermocouple wire for continuous temperature monitoring. Either decamethylferrocene or ferrocene was used as a potential reference.

General Procedure for Oxidation of Aza-thia[7]helicene 1 with $[NO]^+[PF_6]^-$ to Radical Cation $\mathbf{1}^{\bullet+}PF_6^-$ and Aminyl Radical $\mathbf{1}^{\bullet}$. *Oxidation of 1.* [7]Helicene **1** (0.4−0.6 mg) and a Teflon coated magnetic microbar were dried under high vacuum overnight in the Schlenk compartment. In selected experiments, cesium carbonate (6−15 equiv) was added to [7]helicene, prior to drying under vacuum. $[NO]^+[PF_6]^-$ (≥20 equiv) was weighed inside an argon-filled glovebox and then transferred to the Schlenk compartment inside the glovebox. After the two solids came in contact with each other, a dark greenish color appeared. The vessel was transferred from the glovebox to the high-vacuum line, and then dichloromethane was vacuum transferred to the EPR tube. In the EPR-only experiments, stirring was typically carried out at low temperatures such as 195 K (−78 °C), and the EPR spectra were typically obtained at low temperature, 213 or 223 K. In the EPR/UV−vis-NIR experiments, the DCM was vacuum transferred to the UV−vis-NIR cell, and the baseline for the UV−vis-NIR spectra was obtained.[2] Subsequently, the DCM was vacuum transferred to the Schlenk compartment, the vacuum stopcock of the reaction vessel was closed (under vacuum, without argon gas fill), and then the reaction mixture was briefly stirred at room temperature. Subsequently, the reaction solution was consecutively decanted to the EPR tube (or the UV−vis-NIR cell); the EPR spectra (or UV−vis-NIR spectra) were consecutively recorded.[2]

Oxidation of the Anion of 1 Generated with NaH. NaH (4.70 mg, 60% dispersion in mineral oil) was placed in a Schlenk vessel and washed with pentane (5 × 0.5 mL) to remove mineral oil, and then the gray solid was evacuated overnight at room temperature. To the starting material **1** (1.24 mg, 1.75 μmol) in another Schlenk vessel, evacuated on vacuum line at 70 °C overnight, DCM (0.9 mL) was added via vacuum transfer to get a light yellow solution, which was then transferred to the NaH-containing Schlenk vessel under flow of argon. The mixture was stirred at room temperature for 2 h to get a cloudy light brown solution followed by the addition of CH_3CN (0.2 mL) by vacuum transfer. The mixture was stirred for another 20 min until no bubbles formed, to get a clear light brown solution, 200 μL of which was transferred to the Schlenk vessel preloaded with DCM (0.5 mL) and equipped with a side arm 4 mm EPR tube. (The remaining portion of the reaction mixture was used for electrochemical study, described in section 2c, SI.) The solution in the EPR Schlenk vessel (0.4 mM anion of **1** in DCM/MeCN (20:1)) was poured into the side arm EPR tube, and then ferrocenium hexafluorophosphate (3.44 mg, 10.39 μmol) was added through a paper funnel to the Schlenk compartment under argon flow. Then, the solution was poured back to the Schlenk compartment and stirred a total of 10 min (Figure 5).

Oxidation of the Anion of 1 Generated with LDA. To the solution of aza-thia[7]helicene **1** (0.660 mg, 0.935 μmol) in THF (0.14 mL, added by vacuum transfer) was added LDA solution in THF (0.223 M, 7.0 μL, 1.56 μmol) at −20 °C, and then the mixture was stirred at −20 °C for 1 h to form a very light yellow solution. Subsequently, the reaction mixture was cooled to −78 °C with acetone−dry ice bath, and the oxidant, ferrocenium hexafluorophosphate (0.81 mg, 2.45 μmol), was added as a solid via a weighing paper funnel under the flow of argon gas. Then, the reaction mixture was stirred at −78 °C for 1 h to form a dark-brown solution, which was diluted with DCM (added by vacuum transfer to total volume of 0.48 mL).

■ ASSOCIATED CONTENT

Supporting Information

. The Supporting Information is available free of charge on the ACS Publications website at DOI: 10.1021/jacs.6b01498.

General procedures and materials, additional experimental details, and complete ref 23 (PDF)

X-ray crystallographic files for **1** (CIF)

■ AUTHOR INFORMATION

Corresponding Author

*arajca1@unl.edu

Author Contributions

§Y.W. and H.Z. contributed equally to this work.

Notes

The authors declare no competing financial interest.

■ ACKNOWLEDGMENTS

We thank the NSF Chemistry Division for support of this research under Grant No. CHE-1362454.

■ REFERENCES

(1) Shen, Y.; Chen, C.-F. *Chem. Rev.* **2012**, *112*, 1463−1535.

(2) Zak, J. K.; Miyasaka, M.; Rajca, S.; Lapkowski, M.; Rajca, A. *J. Am. Chem. Soc.* **2010**, *132*, 3246−3247.

(3) Ueda, A.; Wasa, H.; Suzuki, S.; Okada, K.; Sato, K.; Takui, T.; Morita, Y. *Angew. Chem., Int. Ed.* **2012**, *51*, 6691−6695.

(4) Sørensen, T. J.; Nielsen, M. F.; Laursen, B. W. *ChemPlusChem* **2014**, *79*, 1030−1035.

DOI: 10.1021/jacs.6b01498
J. Am. Chem. Soc. 2016, 138, 7298−7304

(5) Ravat, P.; Šolomek, T.; Rickhaus, M.; Häussinger, D.; Neuburger, M.; Baumgarten, M.; Juríček, M. *Angew. Chem., Int. Ed.* **2016**, *55*, 1183−1186.
(6) (a) Miyasaka, M.; Rajca, A.; Pink, M.; Rajca, S. *J. Am. Chem. Soc.* **2005**, *127*, 13806−13807. (b) Rajca, A.; Rajca, S.; Pink, M.; Miyasaka, M. *Synlett* **2007**, *2007*, 1799−1822.
(7) Miyasaka, M.; Pink, M.; Rajca, S.; Rajca, A. *Angew. Chem., Int. Ed.* **2009**, *48*, 5954−5957.
(8) Miyasaka, M.; Pink, M.; Olankitwanit, A.; Rajca, S.; Rajca, A. *Org. Lett.* **2012**, *14*, 3076−3079.
(9) Kötzner, L.; Webber, M. J.; Martinez, A.; De Fusco, C.; List, B. *Angew. Chem., Int. Ed.* **2014**, *53*, 5202−5205.
(10) Hua, W.; Liu, Z.; Duan, L.; Dong, G.; Qiu, Y.; Zhang, B.; Cui, D.; Tao, X.; Cheng, N.; Liu, Y. *RSC Adv.* **2015**, *5*, 75−84.
(11) Mori, K.; Murase, T.; Fujita, M. *Angew. Chem., Int. Ed.* **2015**, *54*, 6847−6851.
(12) Licandro, E.; Cauteruccio, S.; Dova, D. *Adv. Heterocycl. Chem.* **2016**, *118*, 1−46.
(13) Williams, P. E.; Jankiewicz, B. J.; Yang, L.; Kenttämaa, H. I. *Chem. Rev.* **2013**, *113*, 6949−6985.
(14) Sugawara, T.; Komatsu, H.; Suzuki, K. *Chem. Soc. Rev.* **2011**, *40*, 3105−3118.
(15) Gryn'ova, G.; Marshall, D. L.; Blanksby, S. J.; Coote, M. L. *Nat. Chem.* **2013**, *5*, 474−481.
(16) Gryn'ova, G.; Coote, M. L. *J. Am. Chem. Soc.* **2013**, *135*, 15392−15403.
(17) Franchi, P.; Mezzina, E.; Lucarini, M. *J. Am. Chem. Soc.* **2014**, *136*, 1250−1252.
(18) Gryn'ova, G.; Coote, M. L.; Corminboeuf, C. *WIREs Comput. Mol. Sci.* **2015**, *5*, 440−459.
(19) Rajca, A.; Miyasaka, M.; Pink, M.; Wang, H.; Rajca, S. *J. Am. Chem. Soc.* **2004**, *126*, 15211−1522.
(20) (a) Miyasaka, M.; Pink, M.; Rajca, A.; Rajca, S. *Chem. - Eur. J.* **2004**, *10*, 6531−6539. (b) Miyasaka, M.; Rajca, A. *J. Org. Chem.* **2006**, *71*, 3264−3266. (c) Rajca, A.; Miyasaka, M.; Pink, M.; Xiao, S.; Rajca, S.; Das, K.; Plessel, K. *J. Org. Chem.* **2009**, *74*, 7504−7513.
(21) Cicchi, S.; Bonanni, M.; Cardona, F.; Revuelta, J.; Goti, A. *Org. Lett.* **2003**, *5*, 1773−1776.
(22) ^{15}N chemical shifts are computed for **1** at the B3LYP/6-31G(d,p)/IEF-PCM-UFF-optimized geometries in chloroform.
(23) Frisch, M. J.; et al. *Gaussian 09*, revision A.01; Gaussian, Inc.: Wallingford, CT, 2009.
(24) Because of expected low pK_a for radical cation and diradical dication of **1** (see ref 29), we may not strictly exclude the possibility that the second wave corresponds to diradical cation ($\mathbf{1}^{2\bullet+}$), that is, deprotonated diradical dication ($\mathbf{1}^{2\bullet 2+}$).
(25) Connelly, N. G.; Geiger, W. E. *Chem. Rev.* **1996**, *96*, 877−910.
(26) Gerson, F.; Huber, W. *Electron Spin Resonance Spectroscopy of Organic Radicals*; Wiley-VCH: Weinheim, Germany, 2003; pp 99−101.
(27) Bäuerle, P.; Segelbacher, U.; Gaudl, K.-U.; Huttenlocher, D.; Mehring, M. *Angew. Chem., Int. Ed. Engl.* **1993**, *32*, 76−78.
(28) Mishra, A.; Ma, C.-Q.; Bäuerle, P. *Chem. Rev.* **2009**, *109*, 1141−1276.
(29) Bordwell, F. G.; Zhang, X.-M.; Cheng, J.-P. *J. Org. Chem.* **1993**, *58*, 6410−6416.
(30) (a) Klingler, R. J.; Kochi, J. K. *J. Phys. Chem.* **1981**, *85*, 1731−1741. (b) This value of $E_p^a - E_p^c$ is not corrected for uncompensated resistance (for corrected values of $E_p^a - E_p^c$, see Table S4, SI). Plot of E_p^a vs. log ν, where ν is the scan rate, is linear with a slope of about 90 mV, that is, it is significantly larger than 30 mV, as expected for an electrochemically irreversible one-electron transfer process (Figure S5, SI).
(31) Thangavel, A.; Rawashdeh, A. M. M.; Sotiriou-Leventis, C.; Leventis, N. *Org. Lett.* **2009**, *11*, 1595−1598. (b) If the typical attenuation factor of 10 nm^{-1} is assumed, $k_s \approx 7 \times 10^{-7}$ cm s^{-1} could correspond to the electron transfer through a pathway of the order of 1 nm, an approximate dimension of the [7]helicene molecule.
(32) (a) Jacquemin, D.; Perpéte, E. A.; Ciofini, I.; Adamo, C. *Acc. Chem. Res.* **2009**, *42*, 326−334. (b) TD-DFT computation for $\mathbf{1}^{\bullet}$, using M06-HF density functional, did not converge.
(33) B97D: Grimme, S. *J. Comput. Chem.* **2006**, *27*, 1787−1799.
(34) ωB97xD: Chai, J. D.; Head-Gordon, M. *Phys. Chem. Chem. Phys.* **2008**, *10*, 6615−6620.
(35) M06-2X and M06-HF: Zhao, Y.; Truhlar, D. G. *Theor. Chem. Acc.* **2008**, *120*, 215−241.
(36) CAM-B3LYP: Yanai, T.; Tew, D.; Handy, N. *Chem. Phys. Lett.* **2004**, *393*, 51−57.
(37) Borden, W. T.; Davidson, E. R. *J. Am. Chem. Soc.* **1977**, *99*, 4587−4594.
(38) Gallagher, N.; Olankitwanit, A.; Rajca, A. *J. Org. Chem.* **2015**, *80*, 1291−1298.
(39) In cyclic voltammetry on anion of **1** (generated with NaH or KH in acetonitrile/DCM or in THF) and using a Pt-working electrode produced, we could not observe a well-defined second oxidation wave that would correspond to $\mathbf{1}^{2\bullet+}$ (Table S4, footnote d, Figure S5 and S6, SI).
(40) Falvey, D. E., Gudmundsdottir, A. D., Eds.; *Nitrenes and Nitrenium Ions*; Wiley-VCH: New York, 2013; pp 1−606.
(41) Gibson, T.; Greene, J. P.; Berkowitz, J. *J. Chem. Phys.* **1985**, *83*, 4319−4328.
(42) Winter, A. H.; Falvey, D. E.; Cramer, C. J.; Gherman, B. F. *J. Am. Chem. Soc.* **2007**, *129*, 10113−10119.
(43) Janke, R. H.; Haufe, G.; Wurthwein, E.-U.; Borkent, J. H. *J. Am. Chem. Soc.* **1996**, *118*, 6031−6035.
(44) Accelerated aging tests for optoelectronic devices are typically carried out at 70 or 85 °C for 2000−5000 h, for example, based upon Telcordia (Bellcore) standards GR-468-CORE.
(45) Rajca, A.; Miyasaka, M. In *Functional Organic Materials - Syntheses and Strategies*; Mueller, T. J. J., Bunz, U. H. F., Eds.; Wiley-VCH: New York, 2007; pp 543−577.
(46) Naaman, R.; Waldeck, D. H. *Annu. Rev. Phys. Chem.* **2015**, *66*, 263−281.
(47) Xu, X.; Li, W.; Zhou, X.; Wang, Q.; Feng, J.; Tian, W. Q.; Jiang, Y. *Phys. Chem. Chem. Phys.* **2016**, *18*, 3765−3771.
(48) *SAINT V7.68A, 2011*, Bruker Analytical X-Ray Systems, Madison, WI.
(49) An empirical correction for absorption anisotropy: Blessing, R. *Acta Crystallogr., Sect. A: Found. Crystallogr.* **1995**, *51*, 33−38.
(50) Burla, M. C.; Caliandro, R.; Carnalli, M.; Carrozzini, B.; Cascarano, G. L.; De Caro, L.; Giacovazzo, C.; Polidori, G.; Sagna, R. *Sir2004, A Program for Automatic Solution and Refinement of Crystal Structure*, Version 1.0, 2004.
(51) SHELXL-97: (a) *SHELXTL-Plus*, Version 2008/4, Bruker Analytical X-Ray Systems, Madison, WI. (b) Sheldrick, G. M. *Acta Crystallogr., Sect. A: Found. Crystallogr.* **2008**, *64*, 112−122.
(52) Spagnol, G.; Rajca, A.; Rajca, S. *J. Org. Chem.* **2007**, *72*, 1867−1869.
(53) Vale, M.; Pink, M.; Rajca, S.; Rajca, A. *J. Org. Chem.* **2008**, *73*, 27−35.
(54) Rajca, A.; Utamapanya, S. *J. Am. Chem. Soc.* **1993**, *115*, 2396−2401.
(55) Rajca, A.; Shiraishi, K.; Vale, M.; Han, H.; Rajca, S. *J. Am. Chem. Soc.* **2005**, *127*, 9014−9020.

DOI: 10.1021/jacs.6b01498
J. Am. Chem. Soc. 2016, 138, 7298−7304